J Mater Sci (2019) 54:6393–6400

Electronic materials

Structural evolution and electrical properties of metal ion-containing polydopamine

Haoqi Li[1], Tim Marshall[2], Yaroslav V. Aulin[2], Akila C. Thenuwara[2], Yao Zhao[1], Eric Borguet[2], Daniel R. Strongin[2], and Fei Ren[1,*]

[1] Department of Mechanical Engineering, Temple University, Philadelphia, PA 19122, USA
[2] Department of Chemistry, Temple University, Philadelphia, PA 19122, USA

Received: 17 September 2018
Accepted: 5 January 2019
Published online: 10 January 2019

© Springer Science+Business Media, LLC, part of Springer Nature 2019

ABSTRACT

Polydopamine (PDA) is a biopolymer that can be synthesized under mild conditions. Thermal annealing can convert PDA into a conductive phase, the so-called carbonized PDA (cPDA). This work studied the effect of three metal ions, i.e., Cu^{2+}, Mg^{2+}, and Na^{+}, on the synthesis of PDA and its conversion to cPDA. Both Cu^{2+} and Mg^{2+} could interact with PDA, which in turn influenced (1) the growth of PDA thin film, (2) morphology change of PDA particles upon thermal annealing, and (3) the electrical properties of heat-treated thin films. In contrast, the presence of Na^{+} ion during the synthesis of PDA did not show any effect. In this study, the morphology of PDA thin films and powder particles was examined using SEM and TEM; their chemical compositions were studied by EDS and ICP-MS; the structure was investigated using electron diffraction and Raman spectroscopy; and the properties were evaluated with respect to the electrical conductivity and thermoelectric Seebeck coefficient. The results from this work provide a potential approach to control the structure and properties of PDA and cPDA materials through metal ion doping.

Introduction

Polydopamine (PDA) is considered a biopolymer inspired by the mussel chemistry [1]. PDA has attracted much attention in recent years due to the ease of its fabrication methods and many interesting properties. PDA can be synthesized through oxidative self-polymerization under mild conditions [1, 2], which can yield nanoscale powders with controllable size [3], or conformal, crack-free thin films on multiple surfaces [4]. The "universal" adhesive behavior of PDA is attributed to the existence of multiple functional groups, e.g., the catechol and amine groups, in the dopamine (DA) molecules. These functional groups allow PDA to interact with other molecules in various ways, such as chelation or hydrogen bonding. Many potential applications of PDA have been proposed, such as surface treatment to modify the hydrophobicity, targeted drug delivery, and capture of heavy metal cations for water treatment [5–8].

Address correspondence to E-mail: renfei@temple.edu

https://doi.org/10.1007/s10853-019-03337-7

PDA can be converted into a carbon-like phase through heat treatment. Carbonized PDA (cPDA) thin films have been found to possess good electrical conductivities as high as 1.2×10^5 S/m [9], which are comparable to reduced graphene oxide (rGO) [1, 10–12]. It is hypothesized that cPDA possessed a structure similar to graphite [13, 14]. The promising electrical conductivity of cPDA makes it a potential candidate for nanostructured carbon material. Compared to graphene or rGO, the fabrication process for cPDA does not involve harsh chemicals and therefore is more environmental friendly. Our previous study [2] showed the formation and growth of nanoscale graphite-like domains in PDA when thermally annealed. While the structure of PDA was primarily amorphous, graphite-like nanostructure started to form at 600 °C, which further grew to approximately 1.5 nm after heat treatment at 900 °C [2]. It was also shown that the electrical conductivity continued to increase with increasing annealing temperature, while the Seebeck coefficient showed the opposite trend.

Some recent studies focused on the interactions between PDA and metal ions to achieve ion-assisted cross-linking in PDA. Introduction of metal ions can alter the structure of PDA network and therefore its properties. For example, Im et al. [15] studied the chelation of Fe^{3+}, Fe^{2+}, Cu^{2+}, and Al^{3+} by the catechol groups in PDA and demonstrated that the metal ions could not only enhance the attachment of the PDA layer on human hair surface, but also increase the overall layer thickness due to increased cross-linking. Kim and coworkers [16] demonstrated immersion of PDA in $FeCl_3$ solution could enhance its stability in strong alkali environment due to the formation of PDA-Fe^{3+} complex. The stability of bonding between organic ligands and metal ions depends on the metal species as well as the oxidation states [17–19]. Monovalent cations such as Na^+ are generally difficult to form coordination bonds and have very low stability constant [18, 19]. Divalent alkaline earth metal ions such as Mg^{2+} bond much easier and have higher stability constants. Cations of transition metals, such as Cu^{2+}, on the other hand, usually form much stronger coordination bonding because of the availability of empty outer shell orbitals that can accept lone-pair electrons [20].

In the current study, Cu^{2+}, Mg^{2+}, and Na^+ cations were introduced during the synthesis of PDA. The electrical properties, including DC and AC conductivities and Seebeck coefficient, were studied and explained with respect to the structure. Our data show different metal ions play different roles in affecting the electrical properties of PDA. This result indicates that doping could be used as a strategy to control the structure and properties of PDA materials, which in turn may be utilized to tune the electrical performance of PDA-based devices in the future.

Experimental method

A base solution was prepared by diluting tris buffer (2 M, Thermo Fisher Scientific Inc., Walthan, MA) to 50 mM with deionized (DI) water and adjusting its pH value to 8.5 using 1 N hydrochloride acid (Thermo Fisher Scientific Inc., Walthan, MA). Substrates either fused silica slides or Si with thermally grown SiO_2 (both from Ted Pella Inc., Redding, CA) were subsequently cleaned with acetone, isopropanol alcohol, and D.I. water in ultrasonication bath. During coating, cleaned substrates were first placed inside the base solution. Dopamine (DA) hydrochloride powder (99%, Alfa Aesar, Haverhill, MA) was then added with a concentration of 2 mg/mL. For each doping experiment, copper chloride ($CuCl_2$), sodium chloride (NaCl), or magnesium chloride ($MgCl_2$), which were purchased from Sigma-Aldrich, St. Louis, MO, was dissolved in the solution with a 1:1 molar ratio between DA molecules and metal ions. The pH of the solution was then readjusted to 8.5 by adding the 2 M tris buffer. After coating, samples were removed and washed with DI water, followed by drying with compressed air, and overnight drying in an oven at 50 °C. In addition to thin film samples, powders were also collected using filer papers after each coating. Carbonization of PDA samples was conducted in a tube furnace under a flowing argon environment between 600 and 900 °C. Heating and cooling rates were set to 5 °C/min with a holding time of 60 min at the peak temperature. To perform electrical measurements, gold electrodes were sputter coated on the thin films.

Surface morphology of the samples was studied using scanning electron microscopy (SEM, FEI Quanta 450 FEG, FEI Inc. Hillsboro, OR) equipped with energy-dispersive x-ray spectroscopy (EDS). Surface roughness and thickness of the film were measured using atomic force microscopy (AFM,

Bruker Demission Icon, Bruker, Billerica, MA). Powder samples are studied with transmission electron microscopy (TEM, JEM 1400, JEOL, Tokyo, Japan). Raman spectroscopy was performed using Horiba LabRAM HR Evolution (Horiba, Japan) with a laser excitation wavelength of 532 nm and spot diameter of 0.72 μm. X-ray photoelectron spectrum (XPS) analysis of the films was carried out using VG Scientific (Thermo Fisher Scientific Inc., Walthan, MA) 100 mm hemispherical analyzer and a Physical Electronics Mg Kα X-ray source operating at 300 W. X-ray diffraction (XRD) was carried out by Bruker D8 discover (Bruker, Billerica, MA) with Cu Kα radiation. Electrical conductivity was calculated from the resistance and sample geometry of the thin films, where the thickness of the thin films was measured using atomic force microscope (Demission Icon, Bruker Corp., Billerica, MA) and the resistance was measured using a Keithley 2750 digital multimeter (Keithley, Cleveland, OH). Electrical impedance was measured using an LCR meter (B&K Precision Corp., Yorba Linda, CA) in the range from 20 Hz to 300 kHz. The Seebeck coefficient was measured using a lab-built apparatus [2]. For each heat treatment condition, at least six samples were included in the measurements, based on which the mean values and standard deviations were calculated. Surface area of the powders was measured by Brunauer–Emmett–Teller (BET) method using Micromeritic ASAP 2020 unit (Micromeritics, Norcross, GA). Metal ion concentration was analyzed by inductively coupled plasma mass spectrometry (ICP-MS) method using Agilent 7900 unit (Agilent, Santa Clara, CA).

Results and discussion

Figure 1 shows the SEM images of PDA coating on Si/SiO_2 substrate. All three types of PDA films doped with Cu^{2+} (Cu-PDA), Mg^{2+} (Mg-PDA), and Na^{+} (Na-PDA) during synthesis appeared to be flat, continuous, and crack free (Fig. 1), which is similar to the surface morphology of undoped PDA thin films [2]. Some bright spots can be observed on all sample surfaces (Fig. 1), which are aggregated PDA particles formed during the synthesis and attached to the film surface. EDS analysis results on the coatings are shown in the insets of Fig. 1. Carbon (C), oxygen (O), and trace amount of nitrogen (N) were observed on all Cu-PDA, Mg-PDA, and Na-PDA samples. Copper

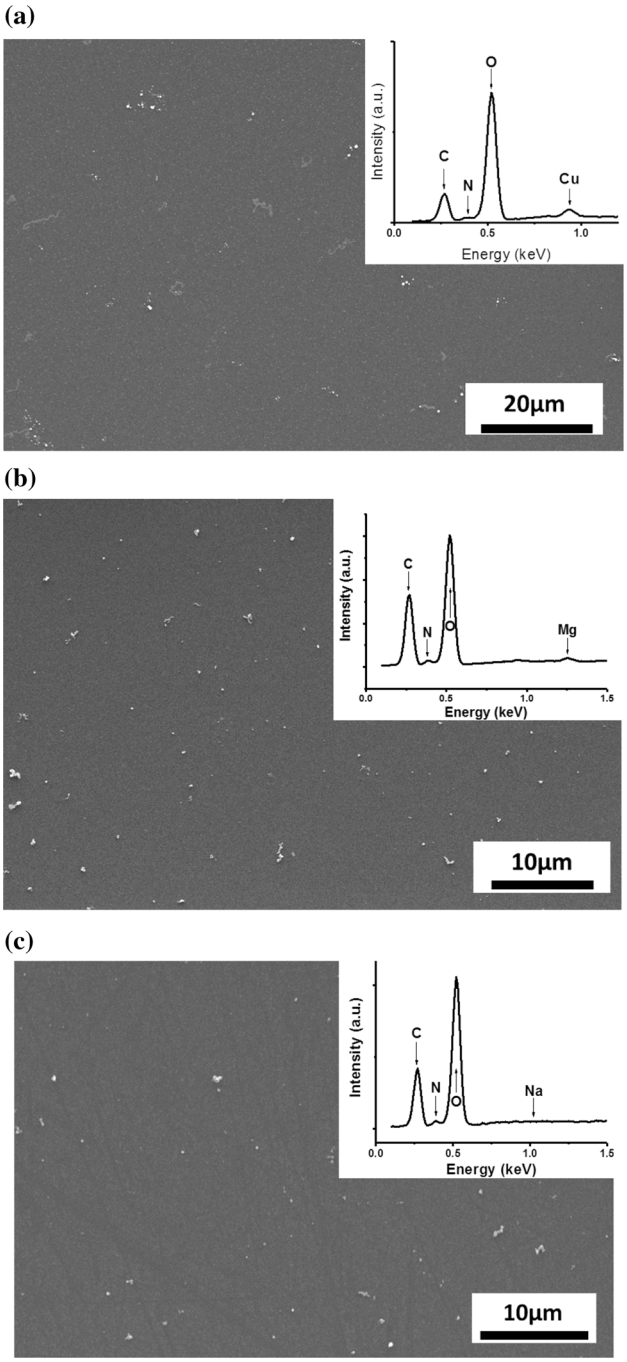

Figure 1 SEM image of **a** Cu-PDA, **b** Mg-PDA, and **c** Na-PDA thin films coated on Si/SiO_2 substrates. Insets show the EDS spectra obtained from areal scans.

(Cu) and magnesium (Mg) peaks were detected on the Cu-PDA (inset of Fig. 1a) and the Mg-PDA (inset of Fig. 1b) samples, respectively. However, sodium (Na) peak was not detected on the Na-PDA sample (inset of Fig. 1c). The concentration of metal ions was further measured using ICP-MS (Table S3), which

showed the molar ratio between Cu and DA was approximately 1:6.1; the ratio between Mg and DA was approximately 1:4.2, and Na was less than 1/15 of DA. Both EDS and ICP-MS results indicate a significant amount of Mg and Cu ions were introduced into PDA during the synthesis. In contrast, few Na^+ ions were retained after cleaning and drying. These results also agree well with the literature observation on the different tendencies to form coordination bonding among monovalent, divalent, and transition metal ions [18–20], as previously discussed in "Introduction" section.

AFM measurements revealed all the PDA films were smooth with low surface roughness on the order of nanometers (Table S1). However, the thickness of the thin films was different. For undoped PDA and Na-PDA, the film thickness increased from approximately 4 nm after 1 h coating to 14 nm after 24 h coating (Table S2). In contrast, the thickness of Cu-PDA and Mg-PDA films did not show significant increase when the coating time increased from 1 h (~ 7–8 nm) to 24 h (~ 7–10 nm) (Table S2). It is unclear why Cu^{2+} and Mg^{2+} ions hindered the growth of PDA thin films in the thickness direction. One possibility is related to the interaction of metal ions with DA monomers or oligomers through coordination bonding. It is commonly believed that the formation of PDA is the result of oligomerization of DA molecules and stacking of the oligomers [5, 21, 22], which relies on the oxidations of the catechol groups to dopamine quinone or semi-quinone that can form coordination bonding with various metal ions [6]. Therefore, Cu^{2+} and Mg^{2+} introduced during the synthesis step may also form coordination bonding with dopamine quinone or semi-quinone [17] and affect the stacking of PDA oligomers.

TEM examination of PDA powders showed the metal ion-doped PDA particles had similar morphology to the undoped powders [2], where the powder particle size ranged between 50 and 200 nm in diameter with quasi-spherical or ellipsoidal shapes (SI). After heat treatment, the Na-PDA powder did not show significant change in morphology (Fig. 2a). This result was expected since EDS and ICP-MS indicated few Na^+ ions were retained in the PDA after cleaning and drying (Fig. 1c). On the other hand, some nanoscale features (dark dots in Fig. 2b) were observed in the Mg-PDA sample. Most of these nanodots were found on the surface of the PDA particles. Figure 2c shows selected area electron diffraction (SAED) pattern obtained from the Mg-PDA sample heat-treated at 800 °C, where both diffraction rings corresponding to Mg and MgO are observed.

Similar nanodots, such as those seen in Fig. 2d, were observed in the Cu-PDA samples after heat treatment. SAED analysis showed these dark dots are likely to be Cu nanocrystals. The two strong diffraction rings in Fig. 2e correspond to the {111} and the {220} planes of Cu. It is interesting to note that the Cu nanocrystals found in samples treated with higher temperatures tended to show larger size. (See examples indicated by circles in Fig. 2f.) Meanwhile, brighter areas (as indicated by arrows in Fig. 2f) were observed in these samples. These brighter areas did not show any diffraction features and are likely pores.

XPS analysis results on the thin film samples are shown in Fig. 3. For Cu-PDA, the presence of the Cu^{2+} satellite peaks indicates the divalent oxidation state of copper (dash line in Fig. 3a). After heat treatment at 800 °C, the strong Cu^{2+} satellite peak disappeared, the amplitude of the weak Cu^{2+} satellite peak reduced, and the 2p peaks shifted toward lower binding energy, which indicate the reduction of Cu^{2+} ions. This result implies the dark inclusions observed in the TEM images of the Cu-PDA particles after heat treatment (Fig. 2d, f) were likely metallic Cu. Similar reduction trend was also observed in the Mg-PDA sample. As shown in Fig. 3b, binding energy of the Mg_{2p} peak shifted from ~ 52 to ~ 50 eV, implying partial reduction of Mg^{2+} to Mg [23, 24]. In contrast, XPS scan did not detect peaks associated with Na or its ions with significant magnitude, which was in agreement with the EDS result (Fig. 1c).

To explore the structure of the PDA phase, Raman spectroscopy measurements were conducted on samples heat-treated between 600 and 900 °C. The D band (~ 1350 cm^{-1}) and the G band (~ 1580 cm^{-1}) were observed on all samples included in this study. The position of the G band blueshifted as the heat treatment temperature increased (Fig. 4a); meanwhile, the intensity ratios between the D bands and G bands (I_D/I_G) of all three samples also increased with increasing heat treatment temperature (Fig. 4b). These results are similar to those reported for undoped PDA [2] and indicate the formation and growth of nanoscale graphite domains [25, 26].

To evaluate the effect of the electrical properties of the PDA thin films, electrical conductivity and

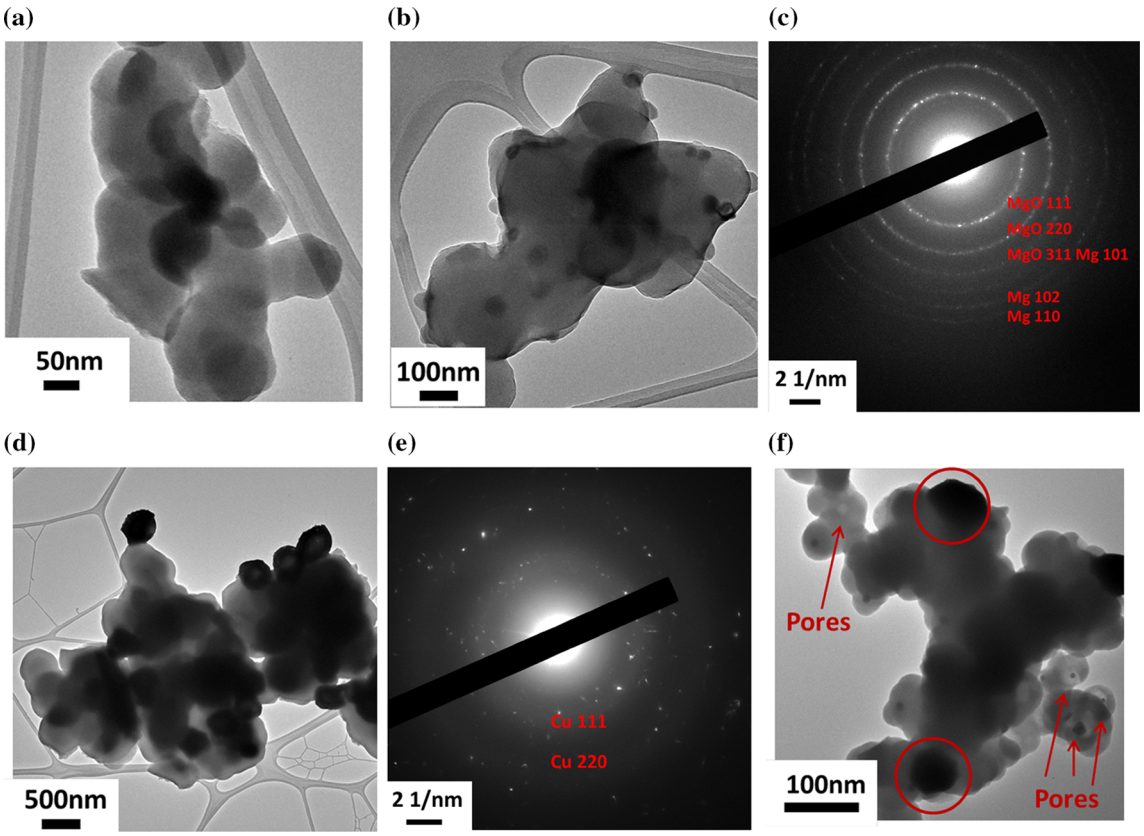

Figure 2 TEM images and selected area electron diffraction (SAED) of cPDA powder samples. **a** TEM image of Na-PDA powder after heat treatment at 800 °C. **b**, **c** TEM image and SAED of Mg-PDA powder after heat treatment at 800 °C. **d**, **e** TEM image and SAED of CU-PDA powder after heat treatment at 700 °C. **f** TEM image of Cu-PDA powder after heat treatment at 1000 °C.

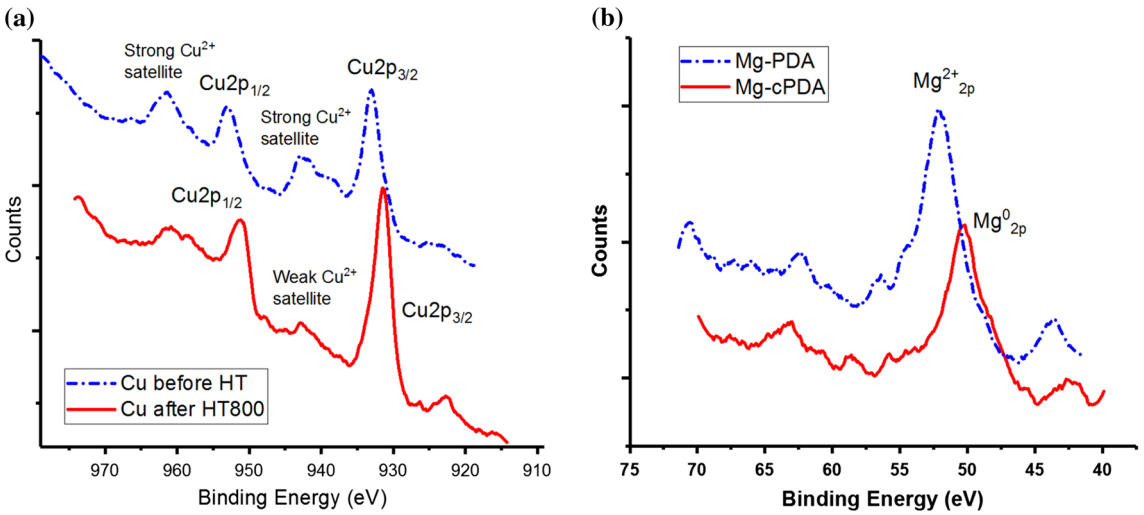

Figure 3 Comparison of XPS spectra of **a** Cu^{2+}-doped PDA **b** Mg^{2+}-doped PDA before and after heat treatment at 800 °C.

Seebeck coefficient were measured at room temperature (Table 1). As heat treatment temperature increases, both the Na-PDA and Mg-PDA samples showed monotonic increase in electrical conductivity and monotonic decrease in Seebeck coefficient, which were similar to the undoped PDA sample (Table 1).

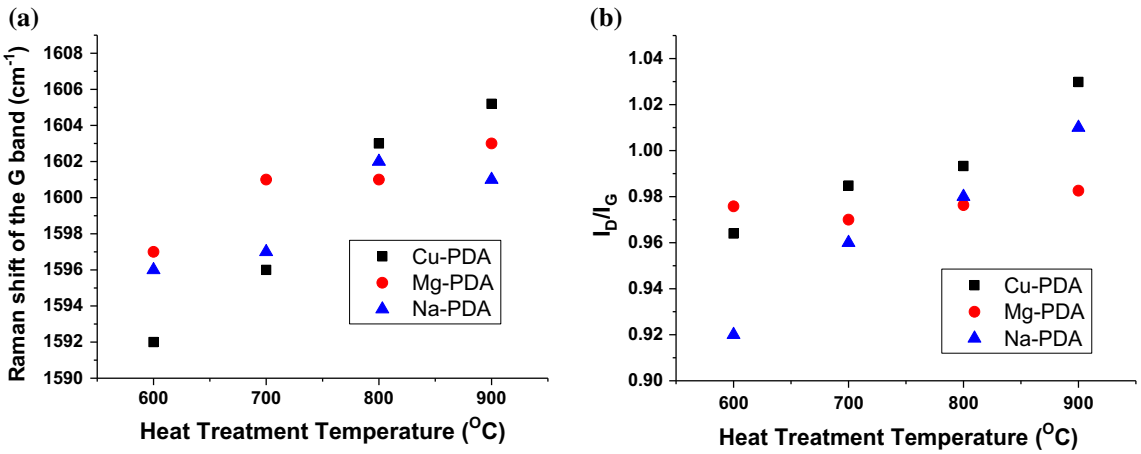

Figure 4 Effect of annealing temperature on **a** the position of the G band and **b** intensity ratio between the D band and the G band. The increasing trends in the two sets of data indicate the conversion from amorphous carbon to nanocrystalline graphite [2, 25, 26] in all metal ion-doped samples.

As shown in our previous work [2], this behavior is expected as the carbonization degree of PDA increases with increasing annealing temperature. As above mentioned, Na^+ was not effectively retained in PDA and therefore did not affect the film formation and the carbonization process. In the case of Mg-PDA, although Mg^{2+} existed in the PDA sample after synthesis, precipitated Mg and MgO nanoparticles might have a small effect on the structure of the PDA phase since they tended to migrate to the surface (Fig. 2b).

On the other hand, Cu-PDA sample showed some different behaviors: The electrical conductivity first increased after annealing at 700 °C and then dramatically decreased when the annealing temperature was beyond 800 °C (Table 1). As a result, the Cu-PDA sample possessed the highest electrical conductivity among all samples thermally annealed at 700 °C, which may be due to the contribution from Cu nanocrystals in the cPDA matrix (Fig. 2d). However, the Cu-PDA samples showed the lowest electrical conductivities after annealing at 800 °C and 900 °C (Table 1). This may be related to the generation of pores in the cPDA matrix as a result of growth of Cu nanoparticles at higher temperatures (Fig. 2f). Meanwhile, the Seebeck coefficient of Cu-PDA samples also exhibited a general trend of decreasing as the annealing temperature increased (Table 1), similar to those observed in undoped and other metal ion-doped PDA samples.

Electrical impedance was also measured between 20 Hz and 300 kHz on samples heat-treated at 600 °C and 800 °C. As shown in (see Fig. S5), the impedance exhibited a sharp drop in 600 °C samples as the frequency increases starting around 5000 Hz and decreased by more than 50% at 300 kHz. In contrast, the impedance of 800 °C samples showed much less decrease as frequency increased, which indicates the non-ohmic contribution to the overall electrical impedance is negligible. The different frequency responses between the 600 °C samples and 800 °C samples are related to the effect of heat treatment on

Table 1 Room temperature electrical conductivity (σ) and Seebeck coefficient (S) of PDA thin films

Annealing temperature (°C)		600	700	800	900
σ (S/m)	Undoped PDA	88 ± 15	$9.9 \pm 0.7 \times 10^2$	$6.9 \pm 1.1 \times 10^3$	$3.8 \pm 0.4 \times 10^4$
	Cu-PDA	160 ± 30	$7.8 \pm 1.4 \times 10^3$	$6.1 \pm 0.2 \times 10^2$	$1.8 \pm 1.3 \times 10^2$
	Mg-PDA	7.9 ± 1.6	$4.5 \pm 1.9 \times 10^2$	$8.2 \pm 1.6 \times 10^3$	$3.7 \pm 0.5 \times 10^4$
	Na-PDA	5.7 ± 3.9	$5.7 \pm 0.9 \times 10^2$	$4.1 \pm 0.2 \times 10^3$	$3.2 \pm 0.2 \times 10^4$
S (μV/K)	Undoped PDA	26 ± 5	9.7 ± 1.2	5.4 ± 0.4	1.6 ± 0.6
	Cu-PDA	21 ± 0.85	7.0 ± 2.0	9.3 ± 3.3	4.7 ± 2.0
	Mg-PDA	3.2 ± 0.3	1.3 ± 0.4	3.7 ± 1.0	1.2 ± 0.2
	Na-PDA	3.0 ± 0.3	10 ± 2.3	5.0 ± 0.9	1.7 ± 0.8

the structural evolution of PDA [2] and metal-doped PDA materials.

Conclusions

Polydopamine (PDA) materials were synthesized in the presence of Cu^{2+}, Mg^{2+}, and Na^{+} ions. Thickness of PDA thin films was reduced when Cu^{2+} and Mg^{2+} were present. After thermal annealing, Cu nanoparticles formed within the PDA matrix, whose growth resulted in larger particle size and porosity in the PDA phase. Upon heating, Mg nanoparticles were observed mainly on the surface of PDA particles with some oxidation. Raman spectroscopy results indicated that the PDA phase was converted from amorphous toward nanocrystalline graphite despite the presence of the metal species. The Cu-PDA sample showed different electrical properties (electrical conductivity and thermoelectric Seebeck coefficient), likely due to the existence of Cu nanoparticles and pores in the PDA matrix. In contrast, Mg-PDA sample exhibited little variation from the undoped PDA.

Acknowledgements

H.L. and F.R. acknowledge the financial support from Temple University faculty start-up fund. The SEM imaging was performed in the CoE-NIC facility at Temple University, which is based on DoD DURIP Award N0014-12-1-0777 from the Office of Naval Research and is sponsored by the College of Engineering. E.B., T.M., and Y.A. acknowledge support as part of the Center for the Computational Design of Functional Layered Materials, an Energy Frontier Research Center funded by the US Department of Energy, Office of Science, Basic Energy Sciences under Award #DE-SC0012575.

Authors' Contribution

H.L. prepared samples and conducted experiments including SEM, AFM, TEM, XRD, TGA, and electrical conductivity and Seebeck coefficient measurements. T.M., Y.V.A., and E.B. conducted the Raman spectroscopy measurements and data analyses. A.T. and D. S. conducted the XPS experiments and provided data analyses. Y.Z. had helped in the experiment on TEM and had intensive discussion with H. L. F.R. designed and guided the project. All authors have contributed to the manuscript revision.

Compliance with ethical standards

Conflict of interest The authors declare no competing interests.

Electronic supplementary material: The online version of this article (https://doi.org/10.1007/s10853-019-03337-7) contains supplementary material, which is available to authorized users.

References

[1] Lee H, Dellatore SM, Miller WM, Messersmith PB (2007) Mussel-inspired surface chemistry for multifunctional coatings. Science 318:426–430. https://doi.org/10.1126/science.1147241

[2] Li H et al (2017) Structure evolution and thermoeelctic properties of carbonized polydopamine thin films. ACS Appl Mater Interfaces 9:6655–6660. https://doi.org/10.1021/acsmi.6b15601

[3] Jiang X, Wang Y, Li M (2017) Selecting water-alcohol mixed solvent for synthesis of polydopamine nano-spheres using solubility parameter. Sci Rep 4:6070. https://doi.org/10.1038/srep06070

[4] Chen Y, Zhao Y, Liang Z (2015) Solution processed organic thermoelectrics: towards flexible thermoelectric modules. Energy Environ Sci 8:401–422

[5] Dreyer DR, Miller DJ, Freeman BD, Paul DR, Bielawski CW (2013) Perspectives on poly(dopamine). Chem Sci 4:3796–3802. https://doi.org/10.1039/c3sc51501j

[6] Liu Y, Ai K, Lu L (2014) Polydopamine and its derivative materials: synthesis and promising applications in energy, environmental, and biomedical fields. Chem Rev 114:5057–5115. https://doi.org/10.1021/cr400407a

[7] Lynge ME, van der Westen R, Postma A, Stadler B (2011) Polydopamine-a nature-inspired polymer coating for biomedical science. Nanoscale 3:4916–4928. https://doi.org/10.1039/c1nr10969c

[8] Brubaker CE, Messersmith PB (2012) The present and future of biologically inspired adhesive interfaces and materials. Langmuir 28:2200–2205. https://doi.org/10.1021/la300044v

[9] Li R, Parvez K, Hinkel F, Feng X, Muellen K (2013) Bioinspired wafer-scale production of highly stretchable carbon films for transparent conductive electrodes. Angew Chem Int Ed 52:5535–5538

[10] Jia Z et al (2017) Electrical and mechanical properties of poly(dopamine)-modified copper/reduced graphene oxide composites. J Mater Sci 52:11620–11629. https://doi.org/10.1007/s10853-017-1307-z

[11] Jia Z et al (2018) Preparation and electrical properties of sintered copper powder compacts modified by polydopamine-derived carbon nanofilms. J Mater Sci 53:6562–6573. https://doi.org/10.1007/s10853-018-2000-6

[12] Zhao Y, Wang H, Qian B, Li H, Ren F (2018) Copper-polydopamine composite derived from bioinspired polymer coating. J Alloys Compd 742:191–198. https://doi.org/10.1016/j.jallcom.2018.01.183

[13] Kong J et al (2012) Highly electrically conductive layered carbon derived from polydopamine and its functions in SnO_2-based lithium ion battery anodes. Chem Commun 48:10316–10318

[14] Ai K, Liu Y, Ruan C, Lu L, Lu G (2013) Sp2 C-dominant Ndoped carbon sub-micrometer spheres with a tunable size a versatile platform for highly efficient oxygen-reduction catalysts. Adv Mater 25:998–1003

[15] Im KM, Kim T, Jeon J (2017) Metal-chelation-assisted deposition of polydopamine on human hair: a ready-to-use eumelanin-based hair dyeing methodology. ACS Biomater Sci Eng 3:628–636. https://doi.org/10.1021/acsbiomaterials.7600031

[16] Kim S, Gim T, Kang S (2014) Stability-enhanced polydopamine coatings on solid substrates by iron(III) coordination. Prog Org Coat 77:1336–1339. https://doi.org/10.1016/j.porgcoat.2014.04.011

[17] Harding MM, Nowicki MW, Walkinshaw MD (2010) Metals in protein structures: a review of their principal features. Crystallogr Rev 16:247–302. https://doi.org/10.1080/0889311X.2010.485616

[18] Flora SJS, Pachauri V (2010) Chelation in metal intoxication. Int J Environ Res Public Health 7:2745–2788. https://doi.org/10.3390/ijerph7072745

[19] Black BC, Huang HW, Cowan AJ (1994) Biological cooridnation chemistry of magnesium, sodium, and potassium ions. Protein and nucleotide binding sites. Coord Chem Rev 135/136:165–202

[20] Brewer DG, Wong PTT, Sears MC (1968) The nature of the coordination bond in metal complexes of substituted pyridine derivatives. III. 4-Methylpyridine complexes of some divalent transition metal ions. Can J Chem 46:3137

[21] Hong S et al (2012) Non-covalent self-assembly and covalent polymerization co-contribute to polydopamine formation. Adv Funct Mater 22:4711–4717

[22] Vecchia NFD et al (2013) Building-block diversity in polydopamine underpins a multifunctional eumelanin-type platform tunable through a quinone control point. Adv Funct Mater 23:1331–1340

[23] Vincent Crist B (2000) Handbook of monochromic xps spectra: the element of negative oxides. Wiley, New York. ISBN: 978-0-471-49265-8

[24] Huang H, Shih W, Lai C (2010) Nonpolar resistive switching in the Pt/MgO/Pt nonvolatile memory device. Appl Phys Lett 96:193505. https://doi.org/10.1063/1.3429024

[25] Ferrari AC, Robertson J (2004) Raman spectroscopy of amorphous, nanostructured, diamond-like carbon, and nanodiamond. Philos Trans R Soc A Math Phys Eng Sci 362:2477–2512. https://doi.org/10.1098/rsta.2004.1452

[26] Ferrari AC (2007) Raman spectroscopy of graphene and graphite: disorder, electron-phonon coupling, doping and nonadiabatic effects. Solid State Commun 143:47–57. https://doi.org/10.1016/j.ssc.2007.03.052